




Single and double photoionization of the Li-like B^{2+} ion: Strong ionization-excitation contributions


A. Müller ^{*}, P.-M. Hillenbrand , S.-X. Wang, and S. Schippers 
I. Physikalisches Institut, Justus-Liebig-Universität Gießen, 35392 Giessen, Germany

S. Reinwardt  and M. Martins 
Institut für Experimentalphysik, Universität Hamburg, 22761 Hamburg, Germany

J. Seltmann 
Deutsches Elektronen-Synchrotron (DESY), 22607 Hamburg, Germany

F. Trinter 
Molecular Physics, Fritz-Haber-Institut der Max-Planck-Gesellschaft, 14195 Berlin, Germany

I. Bray  and D. V. Fursa 
Department of Physics and Astronomy, Curtin University, Perth WA 6845, Australia

A. S. Kheifets 
Research School of Physics, The Australian National University, Canberra ACT 2601, Australia



(Received 10 March 2025; accepted 29 April 2025; published 12 May 2025)

Single and double photoionization of the Li-like $B^{2+}(1s^2 2s^2 S)$ ion were studied both experimentally and theoretically in the energy range from approximately 250–1200 eV. The cross section σ_{23} for net single ionization in that range is dominated by direct removal of one K -shell electron, a process that is described very well by theory. Accordingly, measured yields of B^{3+} photoproducts were normalized to theory to obtain absolute cross sections σ_{23} . Aside from direct single ionization, there are additional contributions to σ_{23} from photoabsorption resonances. The parameters of the Fano profile of the most prominent of these resonances, the triply excited $2s^2 2p^2 P$ state, were calculated by employing the convergent close coupling (CCC) approach and the theoretical results were experimentally verified. Using the normalization procedure obtained from the investigation of single ionization, also the measured yields of B^{4+} product ions could be put on an absolute cross-section scale. The resulting experimental cross section σ_{24} is in good accord with the CCC calculations revealing unexpectedly strong contributions that arise from ionization with excitation of $B^{2+}(1s^2 2s^2 S)$ forming intermediate autoionizing $B^{3+}(n\ell n'\ell')$ levels, which subsequently decay to B^{4+} by Auger-electron emission. In addition, contributions to σ_{24} from resonant excitation of $B^{2+}(n\ell n'\ell' n''\ell'')$ with $n, n', n'' \geq 2$ could be identified. These triply excited resonances with an empty K shell can decay by simultaneous or sequential emission of two electrons and thus contribute to net double photoionization of the parent B^{2+} ion.

DOI: [10.1103/PhysRevA.111.053108](https://doi.org/10.1103/PhysRevA.111.053108)

I. INTRODUCTION

In a joint experimental and theoretical effort, fundamental photoprocesses of few-electron boron ions are investigated in an extended photon-energy range reaching far beyond the K edge of $B^{2+}(1s^2 2s^2 S)$ at 236.495 eV. In particular, multielectron processes and multiply excited states are studied.

In a preceding publication, photoexcitation of double K -vacancy states in He-like B^{3+} ions was investigated [1] and the role of such hollow ionic states in the net single photoionization of $B^{3+}(1s^2 {}^1S)$ and $B^{3+}(1s2s {}^3S)$ ions was explored. Extremely accurate resonance parameters were calculated, with a focus on the determination of resonance energies, which were obtained with uncertainties of less than 1 meV. In a followup paper, direct photo double ionization of B^{3+} was studied and also the single photoionization of H-like B^{4+} was addressed [2].

Photoionization of ions along the boron isonuclear sequence was investigated in previous experiments with sensitivities sufficient to measure cross sections above ≈ 0.5 Mb. Single photoionization of Be-like B^+ was studied at energies between about 20 and 32 eV covering valence-shell excitations [3]. Core excitations of B^+ were investigated at energies

^{*}Contact author: Alfred.Mueller@physik.jlug.de

Published by the American Physical Society under the terms of the [Creative Commons Attribution 4.0 International](https://creativecommons.org/licenses/by/4.0/) license. Further distribution of this work must maintain attribution to the author(s) and the published article's title, journal citation, and DOI.

from 193 to 215 eV, i.e., in the vicinity of the K edge [4]. Single photoionization of B^{2+} involving the K shell was studied in the photon-energy range 199–238 eV [5].

In the present project, the photon-energy range is very much extended and reaches from about 250 eV, the lower limit of photon energies accessible by the undulator at the given energy of the stored electrons, up to approximately five times the K edge. Moreover, the experimental arrangement has reached a sensitivity to the minimum measurable cross sections of the size of a few barns [6]. Under these conditions, a quantum leap towards experimentally accessing complex processes and structures in few-electron ions has been made possible. The preceding two papers [1,2] provide evidence for this achievement in the investigation of single and double photoionization of He-like boron ions.

Here, we report on experiments elucidating higher-order processes and complex multiply excited structures that play a role in the single and double photoionization of Li-like $B^{2+}(1s^2 2s^2 S)$ ions. The experiments were accompanied by theoretical calculations employing the convergent close coupling (CCC) approach [7–10] and a model describing direct photo double ionization (PDI) of atoms and ions by a single photon [11].

Net single photoionization of the ground-level B^{2+} ion, i.e., the total final production of B^{3+} as a consequence of the absorption of a single photon is possible via a number of different pathways. Direct ionization can occur in the L shell or in the K shell:

$$h\nu + B^{2+}(1s^2 2s^2 S) \rightarrow B^{3+}(1s^2 {}^1S) + e^- \quad (1)$$

$$h\nu + B^{2+}(1s^2 2s^2 S) \rightarrow B^{3+}(1s 2s {}^{1,3}S) + e^-. \quad (2)$$

Both channels are characterized by what is usually called the photoeffect. The cross sections for such processes are relatively well known since decades (see, e.g., Ref. [12]). The B^{3+} product after K -shell ionization is in a long-lived excited state ($1s 2s {}^{1,3}S$) that can decay by radiative transitions or reach the final-ion detector in an experiment before relaxing to the ground state. Lifetimes are 10.86 μ s for the 1S [13] and 149 ms for the 3S [14] levels. In any case it is counted as a singly ionized product.

K -shell ionization of B^{2+} may also be accompanied by excitation of one or both of the two other electrons:

$$h\nu + B^{2+}(1s^2 2s^2 S) \rightarrow B^{3+}(1s n\ell) + e^- \quad (3)$$

$$h\nu + B^{2+}(1s^2 2s^2 S) \rightarrow B^{3+}(n\ell n'\ell') + e^-, \quad (4)$$

where $n, n' \geq 2$, and $\ell(\ell') = 0, 1, 2, \dots, n-1(n'-1)$. The singly excited product ion of the process described by Eq. (3) can only decay by photon emission and thus maintains its charge state so that this pathway contributes solely to net single ionization. The situation is much different for the doubly excited product of the ionization-excitation (IE) described by Eq. (4). The $B^{3+}(n\ell n'\ell')$ ion with its empty K shell will most likely decay by an Auger process and has only a very small branching ratio for stabilization of its charge state by radiative transitions. Accordingly, the total process predominantly contributes to net double and, very unlikely, to net single ionization, respectively.

It is commonly accepted and proven by experiment and theory that ionization-excitation as a two-electron or even multielectron process has a much smaller cross section than ionization alone (see, for example, Refs. [1,8,15–17] and references therein). However, we show in this paper that ionization-excitation can make a significant contribution to the cross section for net double ionization.

A third class of photoabsorption processes that can eventually lead to ionization is characterized by K -shell excitation of the parent ion:

$$h\nu + B^{2+}(1s^2 2s^2 S) \rightarrow B^{2+}(1s n\ell n'\ell') \quad (5)$$

$$h\nu + B^{2+}(1s^2 2s^2 S) \rightarrow B^{2+}(n\ell n'\ell' n''\ell''), \quad (6)$$

where $n, n', n'' \geq 2$ and $\ell, \ell', \ell'' = 0, 1, 2, \dots, n-1, n'-1, n''-1$, respectively. The selection rules for electric-dipole transitions suggest that the photoexcited states almost exclusively belong to 2P terms.

Excitation of only the $2s$ electron leads to a state that can only relax by photon emission and thus does not change the charge state of the B^{2+} ion. The excitation of one of the two K -shell electrons [see Eq. (5)] produces an autoionizing state whether the $2s$ electron is also excited or not. The most probable decay of that intermediate state is via an Auger process, which results in the production of a B^{3+} ion, i.e., the whole process contributes to net single ionization. Such reaction paths have been studied previously both experimentally and theoretically [5].

The excitation processes described by Eq. (6) involve the excitation of both K -shell electrons and possibly also the $2s$ electron in addition. The energetically lowest term that can thus be reached is $2s^2 2p^2 P$. Even though the $2s$ electron has not been moved to another subshell in this case, such states with empty K shells are called triply excited. They are also often described as hollow states. Triply excited states of lithium and lithiumlike ions have received a great deal of attention due to their fundamental properties as well as their potentially exotic production and decay processes.

Triply excited states have first been experimentally observed in elastic scattering of electrons from He atoms [18] and were immediately identified spectroscopically as $2s 2p^2 D$ and $2s^2 2p^2 P$ terms of He^- ions [19]. These resonances were also found in the observation channel of electron-impact single ionization of He [20]. In both cases, the triply excited He^- states are formed by trielectronic capture [21,22] of the incident electron. In one case, the intermediate state decays back to the ground state of the He atom by a transition in which two electrons fall down into the K shell while the third electron is emitted with the energy of the incident electron. In the other case, the triply excited states are populated in the same fashion but then decay by a double-Auger process forming a He^+ product ion. Experiments were performed studying exotic triply excited states of He^- populated in beam-foil experiments [23] or via photoabsorption by long-lived metastable He^- ions [24].

While in the above examples the triply excited states were associated with three-electron He^- ions, the first observations of hollow Li atoms were made in electron-spectroscopy experiments with foil-excited lithium [25,26]. A decade later, triply excited levels of the Li atom were populated via

trielelectronic capture by Li^+ ions in an electron-ion crossed-beams experiment. The triply excited resonances were identified by scanning the energy of the narrow-bandwidth incident electrons while observing Li^{2+} product ions emerging from the electron-ion interaction region after the emission of two electrons either simultaneously or in two steps [27]. Mainly in the subsequent decade, a striking number of high-profile publications about experimental and theoretical investigations appeared in the literature illuminating the properties of triply excited states of the lithium atom [28–39] and highlighting the importance of such states in atomic physics. Much more work on the topic has been done and would deserve mentioning. However, a complete overview of the associated literature goes far beyond the intent of the present paper. Instead, we refer to published reviews on triply excited states in the lithium atom [40–42]. Multiple photoionization of atoms and molecules has also been reviewed [43].

In the present context, triply excited lithiumlike ions (rather than the Li atom), and in particular B^{2+} ions, are of immediate interest. Experimental work on triply excited positive ions started with beam-foil experiments [26], which provided energies for a number of triply excited Be^+ states. Triply excited states were observed in electron collisions with He-like N^{5+} and Li^+ [44,45] as well as in collisions of ions with light gases leading to what has been termed resonant transfer excitation associated with Auger-electron emission (RTEA) [46]. Some of the experiments addressing RTEA yielded information about triply excited B^{2+} states [47,48]. Yet another access to triply excited states is provided by spectroscopy of photons emerging from very dense hot plasmas (see Ref. [49] and references therein).

A large volume of results from theoretical investigations of triply excited Li atoms and Li-like ions exists in the literature (see Refs. [50–54] and references therein). Results of the present investigation on B^{2+} ions are compared to calculated data from the cited literature.

This paper is organized as follows. Next to this introduction, in Sec. II, the experimental procedures are outlined. In Sec. III, the theoretical CCC approach to photoionization of B^{2+} and the model calculations for direct two-electron removal are briefly explained. Section IV presents and discusses the theoretical and experimental results. The paper ends with a summary (Sec. V).

II. EXPERIMENT

The experiment was conducted at the soft-x-ray beam line P04 [55] of the synchrotron light source PETRA III [56] operated by DESY in Hamburg, Germany. The permanent end station PIPE (Photon-Ion Spectrometer at PETRA III) [57] of beam line P04 provided the complete experimental setup needed for the present measurements. The photon-ion merged-beams technique [58] was employed. The experimental procedures for the measurement of cross sections at PIPE have been previously described in great detail [59,60]. The present measurements were part of an experimental campaign aiming at photoionization of boron ions. First results and the techniques employed in that campaign have already been published [1,2]. Therefore, the present description of the experimental procedures is kept at a minimum.

Beams of isotopically purified 12-keV $^{11}\text{B}^{2+}$ ions, filtered by a magnetic-dipole analyzer, were collimated to a diameter of about 1 mm and merged with the counterpropagating photon beam provided by beam line P04. Photoionized B^{3+} and B^{4+} product ions were separated from the parent $^{11}\text{B}^{2+}$ ions by a second dipole magnet and then detected with almost 100% efficiency. All parent ions were collected in a large Faraday cup and their electrical current was measured by a sensitive picoammeter. The measured $^{11}\text{B}^{2+}$ ion-beam current I_{ion} in the interaction region was approximately 10 nA. The flux ϕ_{ph} of the transmitted photon beam was recorded by a calibrated photodiode.

A blazed 400-lines/mm grating with Pt coating was used to achieve the highest possible photon flux. Overview measurements were carried out with a monochromator exit-slit width $w_{\text{es}} = 1000 \mu\text{m}$. Regions around resonances were scanned with either $w_{\text{es}} = 400 \mu\text{m}$ or $200 \mu\text{m}$. At a photon energy $E_{\text{ph}} = 500 \text{ eV}$, $w_{\text{es}} = 1000 \mu\text{m}$ resulted in a photon flux $\phi_{\text{ph}} \approx 1.1 \times 10^{14}$ photons/s and $w_{\text{es}} = 400 \mu\text{m}$ gave $\approx 6.2 \times 10^{13}$ photons/s, respectively. At $E_{\text{ph}} = 435 \text{ eV}$, $w_{\text{es}} = 1000 \mu\text{m}$ resulted in a photon flux $\phi_{\text{ph}} \approx 1.2 \times 10^{14}$ photons per/s and $w_{\text{es}} = 200 \mu\text{m}$ gave $\approx 2.8 \times 10^{13}$ photons/s.

With a monochromator exit-slit width $w_{\text{es}} = 1000 \mu\text{m}$ the photon beam had an energy spread of about 700 meV at $E_{\text{ph}} = 500 \text{ eV}$. The photon-energy spread could be reduced to 400 meV by setting $w_{\text{es}} = 400 \mu\text{m}$. At 435 eV, the energy spread was 200 meV for $w_{\text{es}} = 200 \mu\text{m}$. The photon energies were calibrated by employing resonances in the single photoionization of B^{3+} ions [1]. The energy axis for the present ion-yield and cross-section data is accurate within an error margin of $\pm 0.1 \text{ eV}$. The Doppler shift of photon energies by approximately a factor of $1 + v_{\text{ion}}/c = 1.00153$ due to the counterpropagating photon and ion beams was corrected for, considering the ion velocity $v_{\text{ion}} = 4.59 \times 10^5 \text{ m/s}$ and the vacuum speed of light c .

Yields of B^{3+} and B^{4+} ions produced as a result of single-photon absorption by B^{2+} parent ions were recorded in energy-scan measurements covering desired energy ranges between approximately 250 and 1200 eV. The overlap factor of the photon and ion beams was not separately determined and monitored. Nevertheless, the measured yields can be put on an absolute cross-section scale by a suitable normalization function $A_{\text{corr}}(E_{\text{ph}})$. Such normalization functions were determined in the preceding publications on single and double photoionization of B^{3+} ions [1,2]. Under the condition that the collimation of the ion beam and the geometry of the photon beam do not change in time, the overlap factor of the two beams remains constant and the normalization function $A_{\text{corr}}(E_{\text{ph}})$ known from one experiment can be applied to a different yield measurement. For the measurements on B^{2+} and B^{3+} parent ions, which were performed in one experimental campaign the identical collimations were maintained. Thus, the correction function $A_{\text{corr}}(E_{\text{ph}})$ determined previously for single photoionization of B^{3+} can also be applied to the present yields measured for photoionization of B^{2+} ions.

Alternatively, a separate correction function can be derived for the present measurements. The cross section σ_{23} for the single photoionization of B^{2+} is determined by the direct processes described by Eqs. (1) and (2). IE contributions to single ionization [see Eqs. (3) and (4)] have to be expected

to be negligibly small. Resonance contributions to σ_{23} [see Eqs. (5) and (6)] are small and occur only at discrete energies below the double-ionization threshold at 552.463 eV [61]. The cross sections for direct photoionization of the L and K shells of B^{2+} are well known since a long time. In the present case, we employed the calculations by Verner *et al.* [12] to construct the cross section σ_{23} for the single photoionization of B^{2+} . Dividing this cross section by the measured yield function of B^{3+} product ions gives the correction function $A_{\text{corr}}(E_{\text{ph}})$. It turns out that the thus obtained correction function is practically identical to the $A_{\text{corr}}(E_{\text{ph}})$ derived in the accompanying experiments with B^{3+} ions [1,2].

The total uncertainty of the normalization procedure is determined by the relative uncertainties of the calculated cross section σ_{23} and the limitations of reproducibility of experimental conditions. The former is conservatively assumed to be $\pm 10\%$ while the latter is estimated to be $\pm 15\%$ based on the reproducibility of $A_{\text{corr}}(E_{\text{ph}})$ during the experimental campaign. This results in a total systematic uncertainty of cross-section determinations of $\pm 18\%$, which is similar to the typical uncertainty of absolute cross-section measurements that include the measurement of the beam overlap factor.

III. THEORY

A. Convergent close coupling approach

The general application of the CCC method to photoionization problems has been described previously [7–10]. More specifically, in the present context, two-electron photoionization of the lithiumlike B^{2+} ion is treated via nonelastic electron scattering and electron-impact ionization of the heliumlike B^{3+} ion. The problem of two-electron photoionization of the Li atom has been solved in preceding works [62–64].

The CCC treatment of PDI of B^{2+} is very similar. The first stage of this process is photoionization of a core $1s$ electron, which is far more likely than the ionization of the valence $2s$ electron because of the proximity to the nucleus, which has to absorb the recoil momentum. The two remaining atomic electrons $1s2s$ overlap with various discrete states of the B^{3+} ion. These states are represented by the configuration interaction (CI) expansion over pairs of one-electron orbitals.

The ground state of B^{2+} is represented by a multiconfiguration Hartree-Fock (MCHF) expansion

$$\Psi_0(1, 2, 3) = \sum_{n\ell \neq 2s} C_{n\ell} \langle 1||n\ell \rangle \langle 2||n\ell \rangle \langle 3||2s \rangle. \quad (7)$$

The wave function in Eq. (7) includes only pair correlation, i.e., no configurations with all of the three electrons being promoted to vacant states included. Nor does it contain pair correlation between different atomic shells. A one-hole-one-electron excitation from the K shell $1s2s3s$ has no significant effect on the ground-state energy. The nine-term MCHF expansion, which includes $n\ell^2$ configurations with $\ell \leq 3$ and $n \leq 4$ recovers 92% of the correlation energy.

We require the wave function of electron scattering on the He-like ion B^{3+} . For this purpose we use the CCC theory developed for two-electron targets [65,66]. The first step is to obtain a set of Laguerre one-electron basis functions by taking $N_\ell = 27 - \ell$ for $\ell \leq 3$ with exponential falloff $\lambda_\ell = 4$, and

diagonalize the one-electron Hamiltonian of B^{4+} for each ℓ . This results in one-electron B^{4+} wave functions. We then use the lowest-energy $25 - \ell$ functions to generate two-electron configurations for diagonalizing the two-electron Hamiltonian B^{3+} . To ensure a sufficiently accurate ground state, and to allow for autoionization processes, we include $1s$, $2s$, $2p$ orbitals for the inner electron, and all possible combinations for the outer electron. Diagonalization of the B^{3+} Hamiltonian results in a total of 829 two-electron states. These states include one- and two-electron excitation as well as ionization. All of these states are then included in the CCC calculations of the required electron- B^{3+} wave function on a fine energy mesh of incident electron energies. This is a substantial computational task, made easier by requiring just one partial wave of total orbital angular momentum.

B. Knockout PDI model

Direct, or nonsequential, PDI at energies not too far above the threshold is facilitated by two main mechanisms. The first mechanism is a knockout collision of the primary photoelectron with the residual ion. The second, the shake-off process, is relaxation of the ion with the release of a secondary photoelectron. While the sudden shake-off mechanism is most efficient at large photon energies, the knockout process is largely responsible for PDI near the threshold. The complete CCC theory treats both the knockout and shake-off processes on the same footing. A simplified knockout model [11] ignores the shake-off contribution to PDI. Nor does it take into account the two-electron ionization-excitation processes. In such a simplified treatment, the primary photoelectron undergoes an ionizing (e,2e) collision with the ion and the whole of its energy is shared between the two secondary photoelectrons. The application of such a model was found successful in direct double ionization of the $\text{Ar}^+(3p^{-1})$ ion [67]. It was also useful in estimating partial contribution of various PDI channels and evaluating the role of L -shell single and double core-hole production and decay in m -fold ($1 \leq m \leq 6$) photoionization of the Ar^+ ion [6].

IV. RESULTS AND DISCUSSION

A. Single photoionization of B^{2+}

The parent Li-like B^{2+} ions are in their $(1s^2 2s^2 S_{1/2})$ ground level. As indicated by Eqs. (1) and (2), there are two important contributions to the net single-ionization cross section σ_{23} . These contributions result from direct photoionization of the L shell ($\sigma_{23}^{\text{dir-L}}$) and direct photoionization of the K shell ($\sigma_{23}^{\text{dir-K}}$). These cross sections have been calculated previously, e.g., by Verner *et al.* [12]. In Sec. I, the dominance of direct ionization (σ_{23}^{dir}) in net single photoionization has been discussed. Accordingly, in a very good approximation, $\sigma_{23} \approx \sigma_{23}^{\text{dir}} = \sigma_{23}^{\text{dir-L}} + \sigma_{23}^{\text{dir-K}}$. Figure 1 shows cross sections σ_{23} for net single photoionization of the B^{2+} ion. The cross section $\sigma_{23}^{\text{dir-L}}$ for direct photoionization of the $2s$ valence electron is represented by the green dotted line. It is only about 3% of σ_{23} at the K edge and drops very rapidly with increasing photon energy. The dominant contribution to σ_{23} in the present energy region of interest is direct K -shell

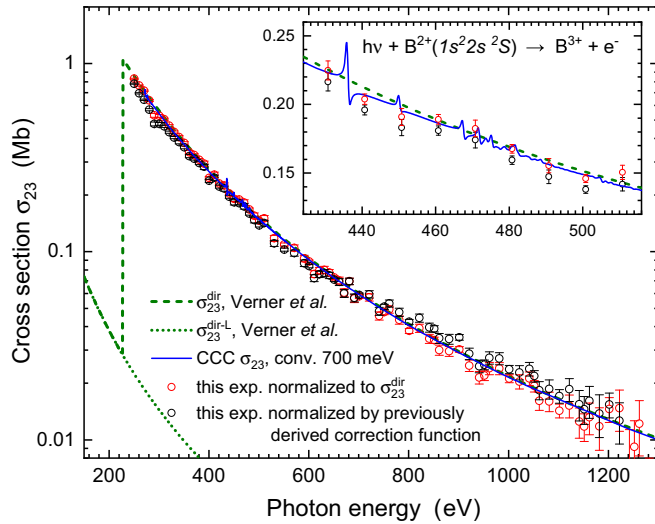


FIG. 1. Theoretical and normalized experimental cross sections σ_{23} for net single photoionization of the B^{2+} ion. The blue solid line is the result of the present CCC calculation after convolution with a Gaussian function of 700 meV FWHM to simulate the experimental conditions. The green dotted line represents the cross section $\sigma_{23}^{\text{dir-L}}$ [12] for direct removal of the $2s$ electron. The green dashed line is $\sigma_{23}^{\text{dir-L}} + \sigma_{23}^{\text{dir-K}}$ for either direct removal of an L -shell or a K -shell electron [12] by a single photon. The present normalized yield data are represented by open red or black circles depending on the method of normalization to an absolute scale. Statistical error bars are shown.

ionization. In Fig. 1, the cross section σ_{23}^{dir} for direct photoionization of B^{2+} is shown as the green dashed line.

The present CCC calculations include all contributions to σ_{23} . In Fig. 1, the CCC cross section for net single ionization is represented by the blue line, which almost perfectly coincides with σ_{23}^{dir} as expected. The inset of Fig. 1 zooms into the energy range of resonance contributions. For a meaningful comparison with the experiment, the theoretical cross section was convoluted with a Gaussian function of 700 meV full width at half-maximum (FWHM). The resonances are relatively small and only the one predicted a few eV below 440 eV has an amplitude that promises experimental accessibility. This resonance is associated with the $2s^2 2p^2 P$ triply excited B^{2+} ion.

The experimental yield data obtained in energy-scan measurements were normalized in two different ways, as described in Sec. II. The red cross-section points in Fig. 1 were obtained by applying a smooth correction function $A_{\text{corr}}(E_{\text{ph}})$ fitted to the ratios of σ_{23}^{dir} and the measured B^{3+} product-ion yields. The black circles with statistical uncertainties in Fig. 1 resulted from the correction function found for the preceding measurements on B^{3+} ions [1] studied in the identical experimental campaign. The two sets of cross sections are in very satisfying agreement and provide evidence for the validity of the chosen normalization procedure. The correction function $A_{\text{corr}}(E_{\text{ph}})$ can thus be applied with good confidence also to the measured yields of B^{4+} products to obtain cross sections σ_{24} for double photoionization of B^{2+} on an absolute scale (see below).

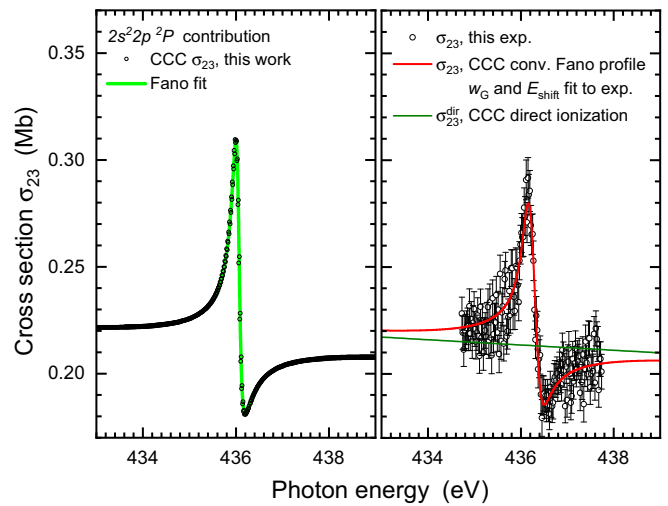


FIG. 2. Cross section σ_{23} for net single photoionization of B^{2+} at energies near the strongest resonance contribution with two K -shell vacancies, $2s^2 2p^2 P$. The left panel shows the results of the present CCC calculations (small open circles) and the result of a Fano fit (light-green solid line) to these points. The right panel presents the normalized experimental data (open circles with statistical error bars) together with a fit to these data (red solid line) by the Gaussian-convoluted Fano profile with the CCC resonance parameters where the Gaussian width w_G and a possible energy shift E_{shift} were used as fit parameters. The almost linear direct-ionization background cross section derived from the present CCC calculations is represented by the green solid line.

An attempt was made to measure the profile of the $2s^2 2p^2 P$ resonance predicted at ≈ 436 eV. The energy range 430–440 eV was explored by scanning the yield of B^{3+} product ions with steps of 0.1 eV. Thus, the rough position of the resonance could be found. Then the monochromator exit slit was gradually closed and finally a production run was performed with $w_{\text{es}} = 200 \mu\text{m}$. The experimental yield resulting from this run was normalized so that the nonresonant background matches the calculated direct photoionization cross section σ_{23}^{dir} . The present experimental and CCC results for the resonance are compared to one another in Fig. 2.

The left panel of Fig. 2 shows the cross section σ_{23} calculated at discrete photon energies together with a Fano profile [68] fitted to the data points. From the fit, the resonance energy is 436.0522(3) eV where the number in parentheses indicates the statistical uncertainty of the last digit resulting from the fit. The absolute uncertainty of the calculated energy is expected to be much greater than 0.3 meV as evidenced by the comparisons shown in the preceding paper on doubly excited resonances in the photoionization of B^{3+} ions. Other parameters obtained from the fit are the Fano parameter $q = -1.69$, the Lorentzian width $\Gamma = 0.177$ eV, and the resonance strength $A = 0.0171$ Mb eV.

The right panel of Fig. 2 shows the normalized experimental cross sections σ_{23} as open circles with statistical error bars. The green solid line is the direct-ionization background σ_{23}^{dir} resulting from the CCC calculations. For comparison with the experimentally determined resonance, a fit curve based on the CCC calculations is shown as a solid red line. The fit curve is

essentially the Fano profile shown by the green line in the left panel of Fig. 2 convoluted with a Gaussian function. Free parameters of the fit were the Gaussian width w_G and a possible energy offset E_{shift} from the theoretical resonance energy. The fit gave $w_G = 0.200(18)$ eV and $E_{\text{shift}} = 0.214(6)$ eV. The Gaussian width matches the energy resolution of the photon beam that was found under the same conditions in the experiments with B^{3+} ions [1] during the identical experimental campaign. The energy shift of 0.214 eV is the deviation of the theoretical resonance energy down from the experiment.

A convoluted Fano profile [69] independent of theory has also been fitted to the measured $2s^22p^2P$ resonance keeping the known energy resolution fixed. The resulting fit curve is almost identical to the red solid line in the right panel of Fig. 2. The resonance energy obtained by that fit is 436.254 eV, whereas the procedure described above results in $(436.052 + 0.214)$ eV = 436.266 eV. The difference is a measure of the uncertainty of the fitting procedures with the given scatter of the experimental cross-section data. Differences of 12 meV are still very small compared to the systematic experimental uncertainty of ± 100 meV of the photon-energy scale.

Photon energies observed during the experimental campaign with boron ions were calibrated to resonance energies known with meV precision [1]. Unfortunately, however, the reproducibility of energy readings during photon-energy scans and the stability of the optical components over time are limited and thus also limit the precision of measured photon energies. Instabilities at beam line P04 have recently been documented [70]. Deviations between the true photon energy and the set energy, which is controlled via the reading of the premirror and grating angles of the monochromator depend on the photon energy and on the specific optical parameters set in an experiment. The uncertainty quoted here for the excitation energy of the $B^{2+}(2s^22p^2P)$ resonance is an estimate based on our experience with measurements in which the photon energy was carefully controlled by dedicated high-resolution observations employing an electron spectrometer for monitoring the photon energy by the measurement of photoelectron energies during scans. The time and effort needed for such a control would require a dedicated separate allocation of beam time and equipment that was beyond the resources available for the present experimental project.

The resonance energy for excitation of the $2s^22p^2P$ term from the $B^{2+}(1s^22s^2S)$ ground level has been determined previously by theoretical calculations. To the best of our knowledge, there are no experimental data available in the literature so far. It is interesting to compare results of previous work with the present findings (see Table I).

The present theoretical result is practically identical with the resonance energy found by Safronova and Bruch [50]. The maximum difference between all theoretical results is 0.81 eV. Considering that the newer data obtained by Safronova and Bruch [50] supersede the older results of Safronova and Senashenko [71], the maximum difference of (calculated) $2s^22p^2P^o$ resonance energies relative to the present experiment reduces to less than 0.33 eV. This is a quite satisfying agreement, which shows that the energy of that triply excited state is fairly well understood theoretically.

Among the theoretical results, only the calculations by Safronova and Bruch provide the energy splitting between

TABLE I. Excitation energy in eV of the $2s^22p^2P^o$ resonance relative to the $B^{2+}(1s^22s^2S)$ ground level. PE is the result from the present experiment whose fit uncertainty is estimated to be 10 meV due to the limited statistical precision of the measured data. A total uncertainty of 0.1 eV is estimated on the basis of difficulties with absolute calibration as indicated in the main text. PT is the present theory result. The numbers to the right are the results of theoretical work from the references given above the numbers.

PE	PT	[71]	[50]	[51]	[53]
436.26(10)	436.05	435.78	436.06	436.42	436.588

the two fine-structure levels of the $^2P^o$ term with 436.05 eV for the $^2P_{1/2}$ level and 436.07 eV for the $^2P_{3/2}$ level. The splitting 0.02 eV is much smaller than the natural width Γ of each fine-structure component. The present CCC theory finds $\Gamma = 0.177$ eV, which means that the two fine-structure components cannot be resolved in an experiment.

B. Double photoionization of B^{2+}

Figure 3 shows an overview scan of the cross section for double photoionization of B^{2+} together with the result of the present CCC calculations convoluted with a FWHM = 700 meV Gaussian function to simulate the photon-energy spread in this measurement. Also shown in the figure are the results of two model calculations [11] for PDI of $B^{2+}(1s^22s)$.

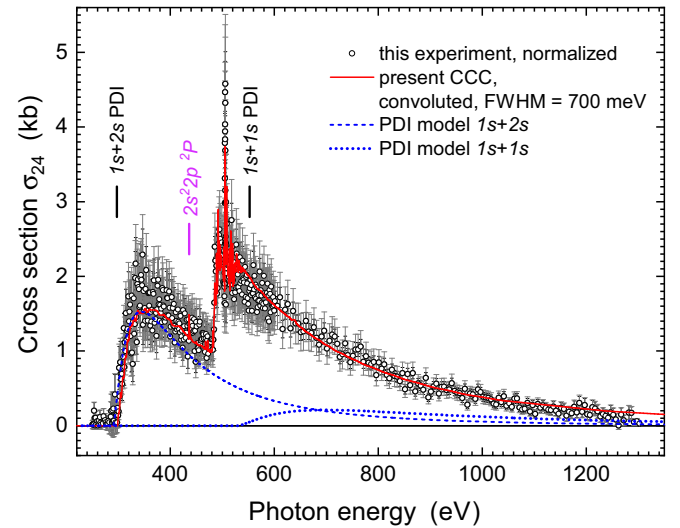


FIG. 3. Cross sections σ_{24} for net double photoionization of B^{2+} . The experimental data are represented by open circles with statistical and total error bars. The theoretical data resulting from the present CCC calculations were convoluted with a Gaussian function of 700 meV FWHM and are represented by the red solid line. The known thresholds for direct removal of one K -shell and one L -shell electron as well as for direct removal of two K -shell electrons by a single photon are indicated by black vertical bars. The position of the $2s^22p^2P$ resonance is indicated by a magenta vertical bar. Cross sections resulting from our model calculations for PDI of the K shell and PDI involving one K - and one L -shell electron are shown by the blue thick dotted and short-dashed lines, respectively.

One (the blue short-dashed line) is the cross section for the direct removal of the $2s$ electron and one of the two $1s$ electrons. The other (the blue thick dotted line) is the cross section for direct double- K -shell ionization. In the range between about 480 and 1000 eV, these partial cross sections can only explain a small part of the net double-ionization cross section σ_{24} . Obviously there are very substantial contributions other than PDI.

As expected, σ_{24} sets in at the threshold energy 297.302 eV [61] for the removal of the $2s$ and a $1s$ electron. The shape of the measured cross section is close to the blue short-dashed line in Fig. 3 representing the $1s + 2s$ PDI calculation. The cross section σ_{24} from the CCC calculations, represented by the red solid curve, closely follows the experiment. It shows a contribution of the $2s^2 2p^2 P$ triply excited state of B^{2+} at 436.052 eV, which must be due to a double-Auger decay. More little spikes are predicted with amplitudes even smaller than that of the leading $2s^2 2p^2 P$ resonance until, all of a sudden, the cross section shows a steep rise above approximately 480 eV. At higher energies, significantly stronger resonance contributions are found by the CCC calculations. Triply excited resonances can be expected in principle up to an energy of 637.528 eV, which is the threshold for the removal of all three electrons from B^{2+} . However, the CCC calculations show resonances dying out below 552.463 eV, which is the threshold for K -shell PDI indicated by a vertical bar in Fig. 3.

The CCC cross section agrees very well with the experiment. Apparently, it comprises all relevant processes that contribute to the net double ionization of B^{2+} . Considering the discussion in Sec. I, contributions of IE may be present in σ_{24} aside from PDI and from the decay of triply excited resonances. In particular, the process described by Eq. (4) that leads to intermediate doubly excited B^{3+} ions may finally produce a B^{4+} double-ionization product ion. IE contributions of specific doubly excited intermediate states can be obtained from the CCC calculations.

As already discussed in a preceding publication [1], the assignment of a spectroscopic notation such as $2s^2 2p^2 P$ to a given resonance is a simplification. In reality, the wave function for describing a physical state is a superposition of basis wave functions. In the specific case of the $2s^2 2p^2 P$ resonance, there is a leading contribution of the $2s^2 2p$ configuration with admixtures of other configurations among which $2p^3$ and $2s2p3s$ may be the most important. In the present CCC calculations, a large number of basis states is involved in the description of the electronic structure and the dynamics relevant to the single and double photoionization of the $B^{2+}(1s^2 2s^2 S)$ ion. Contributions of the basis states to a certain reaction channel can be projected out, however, in most cases such projections say little about the contribution of a real physical state. Exceptions are basis states that make up for a dominating contribution to the wave functions of real states. This is the case for IE channels producing $2\ell 2\ell'$ states by removing one K -shell electron and exciting the second K -shell electron to the L shell.

The $2\ell 2\ell'$ states populated by IE are not subject to selection rules beyond the Pauli principle since the outgoing electron can have different angular momenta and spin orientations and, therefore, it accommodates the production of all

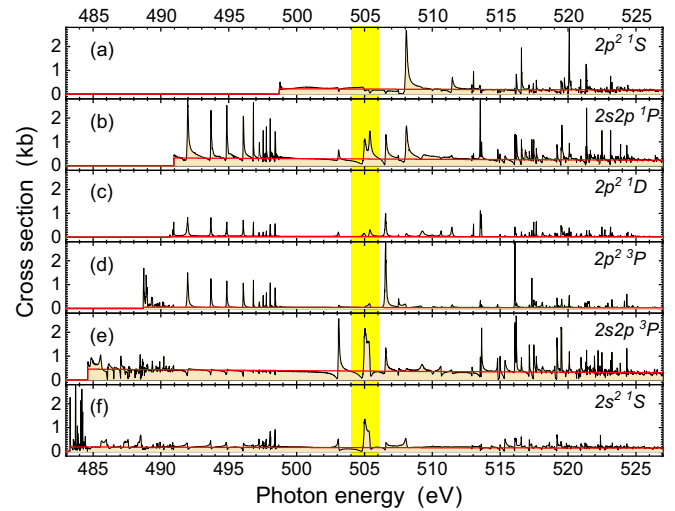


FIG. 4. Cross sections for net ionization plus excitation (IE) producing autoionizing intermediate $B^{3+}(2\ell 2\ell')$ ions ($\ell, \ell' = s, p$) obtained from the present CCC calculations. (a) through (f) show the individual contributions for all terms (specified in the right top corner of each panel) within the doubly excited $2\ell 2\ell'$ manifold of configurations. The cross sections for net IE are represented by the black solid lines with shading. The nonresonant direct-IE contributions are represented by the solid red lines. The energy range 504–506 eV is highlighted by yellow shading. It is the region where the strongest resonance feature occurs in the cross section σ_{24} for net double photoionization of the $B^{2+}(1s^2 2s^2 S)$ ion.

Pauli-allowed terms and levels in the $2\ell 2\ell'$ manifold. Instead of all together ten levels, the present nonrelativistic CCC calculations can only specify the six possible terms ($2s^2 1S$, $2s2p 1P$, $2s2p 3P$, $2p^2 1S$, $2p^2 3P$, and $2p^2 1D$) but not the fine-structure levels. The six possible terms are closely related to six of the basis functions, which contribute predominantly to the wave functions of the six terms. Except for the $2s^2 1S$ and $2p^2 1S$ terms, the selected CCC basis states make up for 93%–100% of the total wave function for the $2\ell 2\ell'$ terms. For the $2s^2 1S$ and $2p^2 1S$ terms the associated basis states make up for about 75% of the total wave functions. It is justified, therefore, to assign the calculated $2\ell 2\ell'$ IE contributions to σ_{24} by associating them directly with the six terms possible within that manifold of configurations.

Figure 4 shows the IE cross sections for the production of intermediate $B^{3+}(2\ell 2\ell')$ ions ($\ell, \ell' = s, p$) obtained from the present CCC calculations. The Figs. 4(a)–4(f) present the contributions of the six terms that are allowed within the $2\ell 2\ell'$ manifold of configurations. The IE cross section for producing intermediate $B^{3+}(2s^2 1S)$ ions has the lowest threshold energy of 483.470 eV [61,72]. There is a smooth contribution $\sigma_{IE}^{dir}(2s^2 1S)$ of direct IE, which is almost constant in the photon-energy range covered by Fig. 4 and there are resonant contributions, which are associated with triply excited B^{2+} states that decay by Auger-electron emission to $B^{3+}(2s^2 1S)$. This in turn relaxes with very high probability by a second Auger decay so that finally two electrons have been released from the initial B^{2+} ion and the whole process of excitation with subsequent sequential Auger decays contributes to net double ionization.

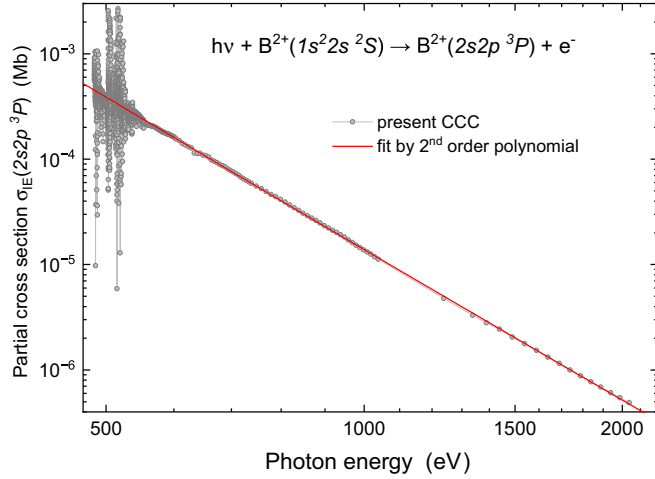


FIG. 5. Partial cross sections $\sigma_{\text{IE}}(2s2p^3P)$ for the net production of intermediate $B^{3+}(2s2p^3P)$ ions resulting from the present CCC calculations in an extended photon-energy range. The theoretical data are represented by small circles. On the double-logarithmic scale the nonresonant part of the cross section can be well represented by a second-order polynomial fit (red solid line).

The most significant IE contribution is shown in Fig. 4(e). It is associated with intermediate doubly excited $2s2p^3P$ states and has a threshold of 484.783 eV [61,72]. A resonance feature is found at about 505 eV both in the $2s2p^3P$ and the $2s^2\ ^1S$ as well as in several other channels. The associated triply excited levels may decay by different Auger processes populating either the intermediate $2s2p^3P$ or $2s^2\ ^1S$ or, in principle, any of the other terms. The energy region around 505 eV is highlighted by yellow shading because the covered resonance features produce the strongest resonance peak in the experimental cross section σ_{24} .

The direct-IE contributions are represented by solid red lines in Fig. 4. They are not explicitly provided by the CCC calculations. For the present purpose they were derived from the energy dependence of the IE cross sections in the region where no resonances can occur. As an example, Fig. 5 shows the CCC result for IE via the $2s2p^3P$ term. A double-logarithmic scale was chosen because in such a plot the nonresonant IE cross sections are almost straight lines and can be very well represented by second-order polynomials. Extension of the polynomial function into the region of resonances delivers the red line for direct IE $\sigma_{\text{IE}}^{\text{dir}}(2s2p^3P)$ provided in Fig. 4(e).

With the theoretical results shown in Fig. 4 and the knowledge of the $1s + 2s$ PDI cross section, the contributions of different reaction channels to the theoretical cross section σ_{24} for net double ionization can be quantified. This is illustrated in Fig. 6. The green solid line with light-green shading represents the contribution of $(1s + 2s)$ PDI. Instead of the blue short-dashed line in Fig. 3, which does not quite match the experimental cross section, a smooth shape function derived by Pattard [73] for representing the shape of photo double ionization cross sections was fitted to the nonresonant low-energy part of the CCC cross section σ_{24} and extrapolated to energies beyond 480 eV.

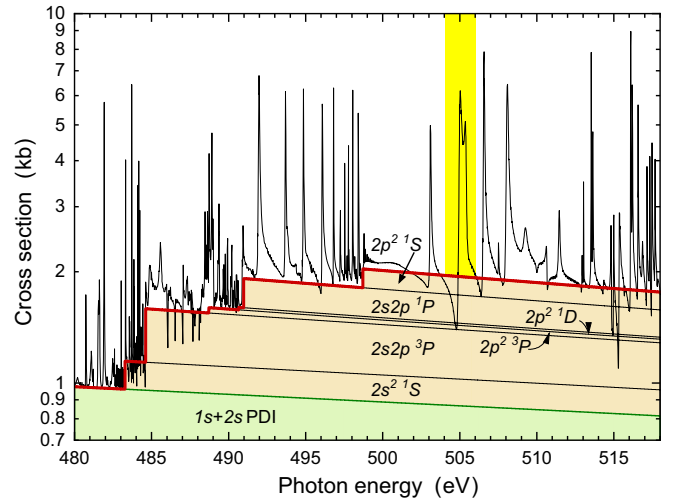


FIG. 6. The CCC cross section σ_{24} for net double photoionization of the $B^{2+}(1s^22s^2S)$ ion is shown as a black solid line in the photon-energy range 480–515 eV. Contributions to σ_{24} from photo double ionization involving a $1s$ and a $2s$ electron (green solid line with light-green shading) and from direct ionization-excitation processes involving the intermediate production of $B^{3+}(2\ell 2\ell')$ ions (light-brown shaded) are indicated. The sum of all nonresonant (direct-ionization) contributions is given by the red solid line. The yellow-shaded energy range is the same as in Fig. 4.

At 483.470 eV [61,72] (483.274 eV in the present CCC calculations), the IE contribution $\sigma_{\text{IE}}(2s^2\ ^1S)$ with the lowest threshold energy sets in, closely followed by the remaining $2\ell 2\ell'$ channels. Figure 6 shows the individual $\sigma_{\text{IE}}^{\text{dir}}(2\ell 2\ell')$ contributions stacked on top of the $(1s + 2s)$ PDI cross section. The total net double-ionization cross section is displayed as a black solid line. In the energy range shown in the figure, this total cross section is the sum of the partial cross sections for $(1s + 2s)$ PDI and IE via autoionizing $2\ell 2\ell'$ states including their resonance contributions. The additional resonances at photon energies below the lowest threshold (483.470 eV) of all IE channels cannot contribute to σ_{24} by sequential Auger decays but only via double-Auger processes, because the population of intermediate autoionizing levels is energetically forbidden. The close-lying thresholds for IE via intermediate $2\ell 2\ell'$ states cause the steep increase of σ_{24} seen in Fig. 3 above a photon energy of approximately 480 eV. It is now clear that this is due to the onset of IE contributions, specifically those proceeding via $2\ell 2\ell'$ autoionizing states. At 500 eV, the calculated total IE contribution is higher than the cross section for direct double ionization by almost a factor 1.3. Obviously, ionization excitation is very important in the net double ionization of Li-like B^{2+} .

On an absolute scale, the sum of all six partial cross sections $\sigma_{\text{IE}}^{\text{dir}}(2\ell 2\ell')$ for K -shell ionization plus K -shell excitation at 500 eV is only 1.1 kb, which, compared to direct straight K -shell ionization with $\sigma_{23}^{\text{dir}-K} \approx 148$ kb at 500 eV, is very small as discussed in Sec. I and as generally expected. Nevertheless, this relatively small cross section can make a major contribution to net double ionization where the competing process of direct double ionization is even smaller. As Fig. 3

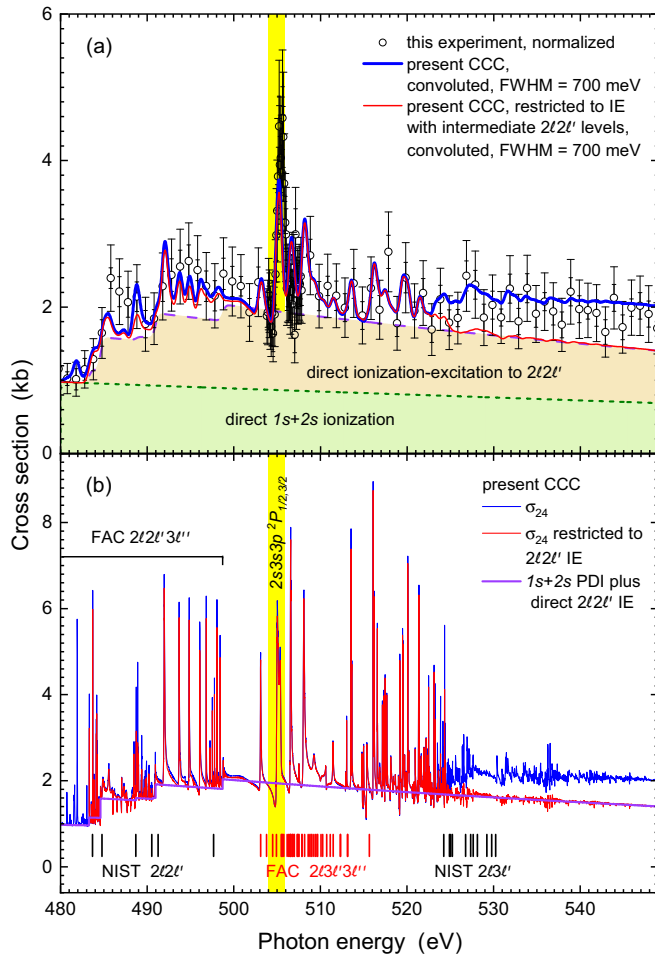


FIG. 7. (a) shows the present experimental cross section σ_{24} for double ionization of B^{2+} (open circles with statistical and total uncertainties) in the photon-energy range 480–549 eV. Also shown are the theoretical cross-section contributions from Fig. 6 convoluted with a FWHM = 700 meV Gaussian function. These data were restricted to contributions of $2\ell 2\ell'$ IE cross sections. The blue line is the total calculated σ_{24} including IE contributions of more highly excited intermediate states. It is convoluted with a Gaussian function of 700 meV FWHM. (b) shows the unconvoluted CCC cross sections from (a) using identical colors. The violet solid line represents the sum of the $1s+2s$ PDI cross section and the (nonresonant) IE contribution to σ_{24} proceeding via $2\ell 2\ell'$ levels. The strongest resonance feature is suggested to be associated with intermediate $B^{2+}(2s3s3p^2P)$ states. It is highlighted by the yellow shading known from preceding figures. The black vertical bars show the energies of $2\ell 2\ell'$ and $2\ell 3\ell'$ levels listed in the NIST spectroscopic database [61]. The red vertical bars were obtained by using the flexible atomic code (FAC) [74] to determine the energy range of $B^{2+}(2\ell 3\ell' 3\ell'')$ resonances. The black horizontal bar extending up to ≈ 500 eV indicates the energy range of $2\ell 2\ell' 3\ell''$ resonances as obtained by employing the FAC code again. This is approximately also the range to be expected for all the $2\ell 2\ell' n\ell''$ resonances.

shows, the cross section for net double ionization is only a few kb at most.

In Fig. 7, the role of IE and IE resonances is illuminated further. The energy range is now 480–549 eV. Figure 7(a) zooms into the experimental spectrum shown in Fig. 3. The

($1s+2s$) PDI contribution is shown as a dashed green line with light-green shading. Stacked on this is the light-brown shaded direct IE contribution via $2\ell 2\ell'$ states. The direct and resonant $2\ell 2\ell'$ contributions were convoluted with a FWHM = 700 meV Gaussian function. Their sum is shown by the red solid line. The total theoretical cross section σ_{24} is convoluted with the same Gaussian function and is shown as the blue solid line in Fig. 7(a). Clearly, a new reaction channel sets in at about 524.3 eV. This is explained by the data shown in Fig. 7(b).

The vertical bars between 480 and 500 eV mark the onsets of IE processes involving $2\ell 2\ell'$ intermediate states. The threshold energies were derived from the NIST tables [61]. The threshold energies found by the present CCC calculations (see the magenta solid line with steps) are almost identical to the NIST energies.

The vertical bars labeled NIST $2\ell 3\ell'$ indicate the thresholds of IE processes involving intermediate $2\ell 3\ell'$ autoionizing states. These energies were also derived from the NIST tables. The red and blue solid lines in Fig. 7(b) are for the identical cross sections as those shown in Fig. 7(a), however, they are not convoluted. Apparently, the mentioned onset of a new reaction channel above 524.3 eV can be attributed to IE processes with autoionizing intermediate $B^{3+}(2\ell 3\ell')$ states.

The strongest resonance feature in the experimental cross section is found at an energy of approximately 505.4 eV. As in the preceding figures, the energy region 504–506 eV is highlighted by yellow shading in both panels. For the purpose of identifying the resonance contributions, atomic-structure calculations were performed employing the flexible atomic code (FAC) [74]. The red vertical bars labeled FAC $2\ell 3\ell' 3\ell''$ show the positions of triply excited resonances with configurations $2\ell 3\ell' 3\ell''$ obtained with the FAC. Clearly, the strongest resonance feature found at about 505 eV belongs to the manifold of $2\ell 3\ell' 3\ell''$ levels and is located near the lowest energy of that manifold. Unfortunately, the results of the FAC calculations are not sufficiently precise to determine exact energies of resonances. For example, the well-known $2s^22p^2P$ resonance discussed in Sec. IV A and in Table I is found by the FAC calculations at 434.53 eV, about 1.7 eV below the present experimental value. Thus, the FAC just provides some guidance for assigning individual resonances. The strongest resonance feature is probably associated with the $2s3s3p^2P_{1/2,3/2}$ doublet. Similarly, the resonances below approximately 500 eV can be associated with configurations $2\ell 2\ell' n\ell''$ with $n \geq 2$.

The energy range 481–507 eV was also scanned with a monochromator exit-slit width $w_{es} = 400 \mu\text{m}$ and with an increased density of points in the range 502–507 eV. The results at energy resolution 400 meV are shown in Fig. 8. The green solid line with light-green shading is the ($1s+2s$) PDI contribution resulting from the present CCC calculations. The stacked light-brown contribution of IE via $2\ell 2\ell'$ states is also obtained from the CCC results as is the red solid line for the total net double-ionization cross section. The experimental data taken with a smaller step size are shown again in the inset together with the FWHM = 400 meV Gaussian-convoluted theoretical σ_{24} (the red solid line) and the unconvoluted σ_{24} (the blue dotted line). The latter is shown to demonstrate that the experimental resonance feature at 505.41 eV

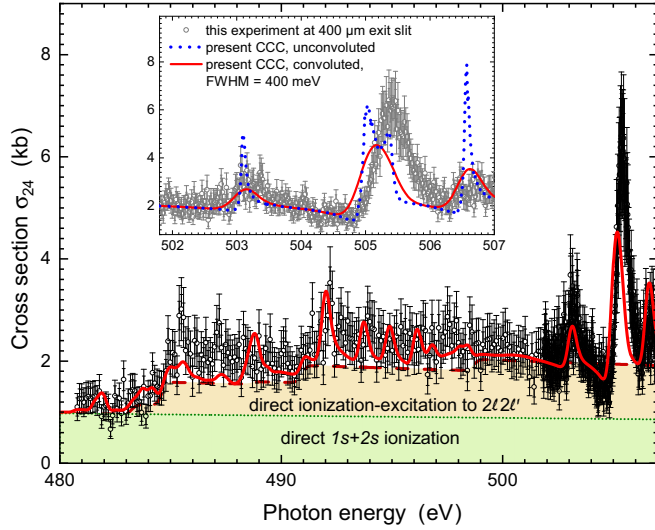


FIG. 8. Comparison of the CCC theory results to an experiment performed with improved energy resolution (400 meV). The inset zooms into the narrow energy range of 501.8–507.0 eV. The open circles with statistical and total error bars represent the experimental data. The red solid line is the result of the CCC calculation of σ_{24} convoluted with a Gaussian function of 400 meV FWHM. The blue dotted line in the inset is the unconvoluted CCC cross section. The reddish-brown long-dashed line is the convoluted contribution of direct IE involving $2\ell 2\ell'$ states sitting on top of the smooth direct-double-ionization cross section involving one K -shell and one L -shell electron.

consists of at least two contributions. According to our FAC calculations the fine-structure splitting of the $2s3s3p^2P$ term is only 9 meV, so that the two components cannot be resolved. The double-peak structure in the unconvoluted CCC results shows an energy separation of about 450 meV, much larger than a possible fine-structure splitting. This might be an indication of additional $2p3s3d^2P$ levels contributing to the cross section σ_{24} . At the given experimental resolution of 400 meV even that structure cannot be resolved. The peak feature at 505.17 eV resulting from convolution of the CCC double-photoionization cross section with a Gaussian function of FWHM = 400 meV is roughly 240 meV below the experimentally observed peak. This deviation is well within the uncertainty of the CCC energy calculations as the shifts of the $2s^22p^2P$ resonance and of the onsets of $\sigma_{\text{IE}}^{\text{dir}}(2\ell 2\ell')$ cross-section contributions show. There are also slight deviations between the sizes of experimental and theoretical resonance features. These deviations may partially be attributed to the uncertainty of the absolute normalization of the experimental cross section and partially also to the statistical uncertainties of the measurements. Energy shifts in theoretically predicted resonance positions may also alter the shape of the convoluted cross section. Apart from these relatively small deviations, theory and experiment are in remarkable agreement.

V. SUMMARY AND CONCLUSIONS

The contribution of ionization-excitation to photoionization cross sections is generally considered to be small. An argument is that the higher-order reaction is much less likely

than the first-order process. Theoretical calculations support this assumption as has been shown again recently for ionization-excitation contributions to straight single ionization of He-like B^{3+} ions by a single photon [1]. The present investigation does not contradict the general assumption. However, the example of double photoionization of Li-like $B^{2+}(1s^22s)$ demonstrates that there are ionization processes in which ionization excitation may even be responsible for a dominant contribution of a given ionization process. In the double photoionization, the direct photo double ionization as a higher-order process already has a relatively small cross section. Hence, the small contribution to double ionization originating from ionization of the K -shell accompanied by excitation of the second K -shell electron to form a doubly excited intermediate product state, which decays by emission of an Auger electron can be substantial relative to the small cross section for direct double ionization. This is exactly what has been found in the present work on photoionization of the Li-like $B^{2+}(1s^22s^2S)$ ion.

Aside from unexpectedly strong contributions of ionization-excitation, also strong contributions of triply excited intermediate states have been observed both in CCC calculations and in experiments on the single and double photoionization of $B^{2+}(1s^22s^2S)$. The relative importance of very highly excited states is usually decreasing with the degree of excitation. This appears to be similar, for example in the cross section for double photoionization at energies up to about 480 eV. However, above the threshold of ionization-excitation processes, resonance contributions are quite important again. The reason for this observation is in the possible decays of the triply excited states that are populated by photoexcitation of the B^{2+} ground level. At energies below ≈ 480 eV, triply excited levels can only contribute to net double ionization if they decay by a double-Auger process. Sequential Auger processes are energetically forbidden, or, in other words, there is no autoionizing B^{3+} level available to those triply excited states to decay to. At excitation energies above ≈ 480 eV, an increasing number of doubly excited levels becomes accessible to which the initial triply excited resonances can decay by Auger-electron emission. Then in a second step a further Auger process populates the final B^{4+} net-double-ionization product. Two sequential Auger processes are usually much more likely than a double-Auger decay so that highly excited triply excited resonances can produce relatively strong contributions to the cross section σ_{24} .

The experimental findings are in very satisfying agreement with the results of the accompanying CCC calculations. The experiments had to deal with quite small cross sections so that statistical uncertainties of the data obtained are relatively large. There is also room for improvement of the accuracy of measured resonance energies. The use of more intense ion beams that will be accessible by employing a more advanced ion source and sufficient time for more measurements will provide the basis for substantially more accurate experimental results in the near future.

ACKNOWLEDGMENTS

We acknowledge DESY (Hamburg, Germany), a member of the Helmholtz Association HGF, for the provi-

sion of experimental facilities. Parts of this research were carried out at beam line P04 of PETRA III. Beam time was allocated for Proposal No. I-20220764. We gratefully acknowledge support from Bundesministerium für Bildung und Forschung provided within the “Verbundforschung” funding scheme (Contracts No. 05K19GU3 and No. 05K19RG3). F.T. acknowledges funding by the Deutsche Forschungsgemeinschaft - Project 509471550, Emmy Noether Programme. M.M. acknowledges funding by Deutsche Forschungsgemeinschaft - Project 510114039. A.S.K., D.V.F., and I.B.

acknowledge the support of the Australian Research Council, the National Computer Infrastructure, and the Pawsey Supercomputer Centre of Western Australia.

DATA AVAILABILITY

The data that support the findings of this article are not publicly available. The data are available from the authors upon reasonable request.

- [1] A. Müller, P.-M. Hillenbrand, S.-X. Wang, S. Schippers, E. Lindroth, F. Trinter, J. Seltmann, S. Reinwardt, M. Martins, A. S. Kheifets, and I. Bray, Double- K -hole resonances in single photoionization of He-like B^{3+} ions, *Phys. Rev. A* **110**, 062802 (2024).
- [2] A. Müller, P.-M. Hillenbrand, S.-X. Wang, S. Schippers, I. Bray, A. S. Kheifets, E. Lindroth, S. Reinwardt, M. Martins, J. Seltmann, and F. Trinter, Direct double ionization of the He-like B^{3+} ion by a single photon, *Phys. Rev. A* **111**, 023115 (2025).
- [3] S. Schippers, A. Müller, B. M. McLaughlin, A. Aguilar, C. Cisneros, E. Emmons, M. F. Gharaibeh, and R. A. Phaneuf, Photoionization studies of the B^+ valence shell: Experiment and theory, *J. Phys. B: At. Mol. Opt. Phys.* **36**, 3371 (2003).
- [4] A. Müller, S. Schippers, R. A. Phaneuf, S. W. J. Scully, A. Aguilar, C. Cisneros, M. F. Gharaibeh, A. S. Schlachter, and B. M. McLaughlin, K -shell photoionization of Be-like boron (B^+) ions: Experiment and theory, *J. Phys. B: At. Mol. Opt. Phys.* **47**, 135201 (2014).
- [5] A. Müller, S. Schippers, R. A. Phaneuf, S. W. J. Scully, A. Aguilar, C. Cisneros, M. F. Gharaibeh, A. S. Schlachter, and B. M. McLaughlin, K -shell photoionization of ground-state Li-like boron ions [B^{2+}]: Experiment and theory, *J. Phys. B: At. Mol. Opt. Phys.* **43**, 135602 (2010).
- [6] A. Müller, M. Martins, A. Borovik, Jr., T. Buhr, A. Perry-Sassmannshausen, S. Reinwardt, F. Trinter, S. Schippers, S. Fritzsche, and A. S. Kheifets, Role of L -shell single and double core-hole production and decay in m -fold ($1 \leq m \leq 6$) photoionization of the Ar^+ ion, *Phys. Rev. A* **104**, 033105 (2021).
- [7] A. S. Kheifets and I. Bray, Calculation of double photoionization of helium using the convergent close-coupling method, *Phys. Rev. A* **54**, R995(R) (1996).
- [8] A. S. Kheifets and I. Bray, Photoionization with excitation and double photoionization of the helium isoelectronic sequence, *Phys. Rev. A* **58**, 4501 (1998).
- [9] I. Bray, D. V. Fursa, A. S. Kheifets, and A. T. Stelbovics, Electrons and photons colliding with atoms: development and application of the convergent close-coupling method, *J. Phys. B: At. Mol. Opt. Phys.* **35**, R117 (2002).
- [10] A. W. Bray, A. S. Kheifets, and I. Bray, Calculation of atomic photoionization using the nonsingular convergent close-coupling method, *Phys. Rev. A* **95**, 053405 (2017).
- [11] A. S. Kheifets, Dynamic scaling of photo-double-ionization to electron impact, *Phys. Rev. A* **101**, 032701 (2020).
- [12] D. A. Verner, D. G. Yakovlev, I. M. Band, and M. B. Trzhaskovskaya, Subshell photoionization cross sections and ionization energies of atoms and ions from He to Zn, *At. Data Nucl. Data Tables* **55**, 233 (1993).
- [13] A. Derevianko and W. R. Johnson, Two-photon decay of $2\ ^1S_0$ and $2\ ^3S_1$ states of heliumlike ions, *Phys. Rev. A* **56**, 1288 (1997).
- [14] G. W. F. Drake, Theory of relativistic magnetic dipole transitions: Lifetime of the metastable 2^3S state of the heliumlike ions, *Phys. Rev. A* **3**, 908 (1971).
- [15] S. Svensson, B. Eriksson, N. Mårtensson, G. Wendin, and U. Gelius, Electron shake-up and correlation satellites and continuum shake-off distributions in x-ray photoelectron spectra of the rare gas atoms, *J. Electron Spectrosc. Relat. Phenom.* **47**, 327 (1988).
- [16] A. V. Nefiodov, Ionization of helium-like ions with excitation of nl states by high-energy photon scattering, *JETP Lett.* **98**, 1 (2013).
- [17] R. Püttner, G. Goldsztejn, D. Céolin, J.-P. Rueff, T. Moreno, R. K. Kushawaha, T. Marchenko, R. Guillemin, L. Journal, D. W. Lindle, M. N. Piancastelli, and M. Simon, Direct observation of double-core-hole shake-up states in photoemission, *Phys. Rev. Lett.* **114**, 093001 (2015).
- [18] C. E. Kuyatt, J. A. Simpson, and S. R. Mielczarik, Elastic resonances in electron scattering from He, Ne, Ar, Kr, Xe, and Hg, *Phys. Rev.* **138**, A385 (1965).
- [19] U. Fano and J. W. Cooper, Identification of energy levels of negative ions, *Phys. Rev.* **138**, A400 (1965).
- [20] J. J. Quémener, C. Paquet, and P. Marmet, Natural line shapes resolved in the ionization yield of He^+ below the $n = 2$ threshold, *Phys. Rev. A* **4**, 494 (1971).
- [21] M. Schnell, G. Gwinner, N. R. Badnell, M. E. Bannister, S. Böhm, J. Colgan, S. Kieslich, S. D. Loch, D. Mitnik, A. Müller, M. S. Pindzola, S. Schippers, D. Schwalm, W. Shi, A. Wolf, and S.-G. Zhou, Observation of trielectronic recombination in Be-like Cl ions, *Phys. Rev. Lett.* **91**, 043001 (2003).
- [22] A. Müller, Electron-ion collisions: Fundamental processes in the focus of applied research, *Adv. At. Mol. Opt. Phys.* **55**, 293 (2008).
- [23] É. J. Knystautas, Observation of a triply excited state in He^- , *Phys. Rev. Lett.* **69**, 2635 (1992).
- [24] R. C. Bilodeau, J. D. Bozek, A. Aguilar, G. D. Ackerman, G. Turri, and N. Berrah, Photoexcitation of He^- hollow-ion resonances: Observation of the $2s2p^2\ ^4P$ state, *Phys. Rev. Lett.* **93**, 193001 (2004).
- [25] R. Bruch, G. Paul, J. Andrä, and L. Lipsky, Autoionization of foil-excited states in Li I and Li II, *Phys. Rev. A* **12**, 1808 (1975).

- [26] M. Rødbro, R. Bruch, and P. Bisgaard, High-resolution projectile Auger spectroscopy for Li, Be, B and C excited in single gas collisions I. Line energies for prompt decay, *J. Phys. B: At. Mol. Phys.* **12**, 2413 (1979).
- [27] A. Müller, G. Hofmann, B. Weissbecker, M. Stenke, K. Tinschert, M. Wagner, and E. Salzborn, Correlated two-electron transitions in electron-impact ionization of Li^+ ions, *Phys. Rev. Lett.* **63**, 758 (1989).
- [28] L. M. Kiernan, E. T. Kennedy, J.-P. Mosnier, J. T. Costello, and B. F. Sonntag, First observation of a photon-induced triply excited state in atomic lithium, *Phys. Rev. Lett.* **72**, 2359 (1994).
- [29] Y. Azuma, S. Hasegawa, F. Koike, G. Kutluk, T. Nagata, E. Shigemasa, A. Yagishita, and I. A. Sellin, New photon-induced triply excited hollow atom states of lithium, *Phys. Rev. Lett.* **74**, 3768 (1995).
- [30] D. Cubaynes, S. Diehl, L. Journal, B. Rouvellou, J.-M. Bizau, S. Al Moussalami, F. J. Wuilleumier, N. Berrah, L. VoKy, P. Faucher, A. Hibbert, C. Blancard, E. Kennedy, T. J. Morgan, J. Bozek, and A. S. Schlachter, First photoexcitation measurements and *R*-matrix calculations of even-parity hollow states in laser-excited lithium atoms, *Phys. Rev. Lett.* **77**, 2194 (1996).
- [31] L. Journal, D. Cubaynes, J.-M. Bizau, S. Al Moussalami, B. Rouvellou, F. J. Wuilleumier, L. VoKy, P. Faucher, and A. Hibbert, First experimental determination and theoretical calculation of partial photoionization cross sections of lithium over the energy region of hollow atomic states, *Phys. Rev. Lett.* **76**, 30 (1996).
- [32] X. Yang, C. G. Bao, and C. D. Lin, Analysis of triply excited states of atoms in hyperspherical coordinates, *Phys. Rev. Lett.* **76**, 3096 (1996).
- [33] S. Diehl, D. Cubaynes, J.-M. Bizau, L. Journal, B. Rouvellou, S. Al Moussalami, F. J. Wuilleumier, E. T. Kennedy, N. Berrah, C. Blancard, T. J. Morgan, J. Bozek, A. S. Schlachter, L. VoKy, P. Faucher, and A. Hibbert, High resolution measurements of partial photoionization cross sections in hollow lithium: A critical comparison with advanced many-body calculations, *Phys. Rev. Lett.* **76**, 3915 (1996).
- [34] S. Diehl, D. Cubaynes, F. J. Wuilleumier, J.-M. Bizau, L. Journal, E. T. Kennedy, C. Blancard, L. VoKy, P. Faucher, A. Hibbert, N. Berrah, T. J. Morgan, J. Bozek, and A. S. Schlachter, Experimental observation and theoretical calculations of Rydberg series in hollow lithium atomic states, *Phys. Rev. Lett.* **79**, 1241 (1997).
- [35] Y. Azuma, F. Koike, J. W. Cooper, T. Nagata, G. Kutluk, E. Shigemasa, R. Wehlitz, and I. A. Sellin, Photoexcitation of hollow lithium with completely empty *K* and *L* shells, *Phys. Rev. Lett.* **79**, 2419 (1997).
- [36] L. B. Madsen, P. Schlagheck, and P. Lambropoulos, Laser-induced transitions between triply excited hollow states, *Phys. Rev. A* **62**, 062719 (2000).
- [37] S. Diehl, D. Cubaynes, H. L. Zhou, L. VoKy, F. J. Wuilleumier, E. T. Kennedy, J. M. Bizau, S. T. Manson, T. J. Morgan, C. Blancard, N. Berrah, and J. Bozek, Angle-resolved photoelectron spectrometry studies of the autoionization of the $2s^2 2p^2 P$ triply excited state of atomic lithium: Experimental results and *R*-matrix calculations, *Phys. Rev. Lett.* **84**, 1677 (2000).
- [38] G. Verbockhaven and J. E. Hansen, Autoionization of triply excited Rydberg series, *Phys. Rev. Lett.* **84**, 2810 (2000).
- [39] L. B. Madsen and K. Mølmer, Correlated electrons in lithium-like hollow atoms, *Phys. Rev. Lett.* **87**, 133002 (2001).
- [40] F. J. Wuilleumier, From doubly excited states of helium to triply excited states of lithium, *Phys. Essays* **13**, 230 (2000).
- [41] E. T. Kennedy, Photogeneration of hollow atoms: Recent developments, *Phys. Scr.* **2001**, 32 (2001).
- [42] L. B. Madsen, Triply excited states: electron-electron correlations in lithium, *J. Phys. B: At. Mol. Opt. Phys.* **36**, R223 (2003).
- [43] R. Wehlitz, Simultaneous emission of multiple electrons from atoms and molecules using synchrotron radiation, *Adv. At. Mol. Opt. Phys.* **58**, 1 (2010).
- [44] A. Müller, A. Borovik, Jr., K. Huber, S. Schippers, D. V. Fursa, and I. Bray, Double-*K*-vacancy states in electron-impact single ionization of metastable two-electron $\text{N}^{5+}(1s2s^3S_1)$ ions, *Phys. Rev. A* **90**, 010701(R) (2014).
- [45] A. Müller, A. Borovik, Jr., K. Huber, S. Schippers, D. V. Fursa, and I. Bray, Indirect contributions to electron-impact ionization of $\text{Li}^+(1s2s^3S_1)$ ions: Role of intermediate double-*K*-vacancy states, *Phys. Rev. A* **97**, 022709 (2018).
- [46] T. J. M. Zouros, Resonant transfer excitation associated with Auger electron emission, in *Recombination of Atomic Ions*, edited by W. G. Graham, W. Fritsch, Y. Hahn, and J. A. Tanis, NATO ASI Series B: Physics, Vol. 296 (Plenum Press, New York, 1992), pp. 271–300.
- [47] M. Zamkov, H. Aliabadi, E. P. Benis, P. Richard, H. Tawara, and T. J. M. Zouros, Absolute cross sections and decay rates for the triply excited $\text{B}^{2+}(2s2p^2\ ^2D)$ resonance in electron-metastable-ion collisions, *Phys. Rev. A* **65**, 032705 (2002).
- [48] T. J. M. Zouros, E. P. Benis, M. Zamkov, C. D. Lin, T. G. Lee, P. Richard, T. W. Gorczyca, and T. Morishita, Investigation of triply excited states of Li-like ions in fast ion-atom collisions by zero-degree Auger projectile electron spectroscopy, *Nucl. Instrum. Methods B* **233**, 161 (2005).
- [49] F. B. Rosmej and C. F. Fontes, Hollow ion atomic structure and x-ray emission in dense hot plasmas, *Matter Radiat. Extremes* **9**, 067202 (2024).
- [50] U. I. Safronova and R. Bruch, Triply excited states of the lithium isoelectronic sequence: $Z = 3 - 54$, *Phys. Scr.* **57**, 519 (1998).
- [51] M. J. Conneely and L. Lipsky, Energy levels and classifications of triply excited states of Li, Be^+ , B^{2+} , and C^{3+} , *At. Data Nucl. Data Tables* **82**, 115 (2002).
- [52] M. Conneely and L. Lipski, Energy levels and classifications of triply excited states of N^{4+} , O^{5+} , F^{6+} , and Ne^{7+} , *At. Data Nucl. Data Tables* **86**, 35 (2004).
- [53] A. K. Roy, Density functional studies on the hollow resonances in the Li-isoelectronic sequence ($Z = 4 - 10$), *J. Phys. B: At. Mol. Opt. Phys.* **38**, 1591 (2005).
- [54] A. S. Safronova, A. Stafford, and U. I. Safronova, Dielectronic satellite spectra from hollow He- and Li-like ion states in fluorine, *J. Quant. Spectrosc. Radiat. Transfer* **331**, 109272 (2025).
- [55] J. Viefhaus, F. Scholz, S. Deinert, L. Glaser, M. Ilchen, J. Seltmann, P. Walter, and F. Siewert, The variable polarization XUV beamline P04 at PETRA III: Optics, mechanics and their performance, *Nucl. Instrum. Methods Phys. Res., Sect. A* **710**, 151 (2013).
- [56] C. G. Schroer, H.-C. Wille, O. H. Seeck, K. Bagschik, H. Schulte-Schrepping, M. Tischer, H. Graafsma, W. Laasch, K. Baev, S. Klumpp, R. Bartolini, H. Reichert, W. Leemans, and E. Weckert, The synchrotron radiation source PETRA III and its future ultra-low-emittance upgrade PETRA IV, *Eur. Phys. J. Plus* **137**, 1312 (2022).

- [57] S. Schippers, T. Buhr, A. Borovik Jr., K. Holste, A. Perry-Sassmannshausen, K. Mertens, S. Reinwardt, M. Martins, S. Klumpp, K. Schubert, S. Bari, R. Beerwerth, S. Fritzsche, S. Ricz, J. Hellhund, and A. Müller, The photon-ion merged-beams experiment PIPE at PETRA III - The first five years, *X-Ray Spectrom.* **49**, 11 (2020).
- [58] R. A. Phaneuf, C. C. Havener, G. H. Dunn, and A. Müller, Merged-beams experiments in atomic and molecular physics, *Rep. Prog. Phys.* **62**, 1143 (1999).
- [59] S. Schippers, S. Ricz, T. Buhr, A. Borovik Jr., J. Hellhund, K. Holste, K. Huber, H.-J. Schäfer, D. Schury, S. Klumpp, K. Mertens, M. Martins, R. Flesch, G. Ulrich, E. Rühl, T. Jahnke, J. Lower, D. Metz, L. P. H. Schmidt, M. Schöffler *et al.*, Absolute cross sections for photoionization of Xe^{q+} ions ($1 \leq q \leq 5$) at the 3d ionization threshold, *J. Phys. B: At. Mol. Opt. Phys.* **47**, 115602 (2014).
- [60] A. Müller, D. Bernhardt, A. Borovik, Jr., T. Buhr, J. Hellhund, K. Holste, A. L. D. Kilcoyne, S. Klumpp, M. Martins, S. Ricz, J. Seltmann, J. Viefhaus, and S. Schippers, Photoionization of Ne atoms and Ne^+ ions near the K edge: Precision spectroscopy and absolute cross-sections, *Astrophys. J.* **836**, 166 (2017).
- [61] A. Kramida, Y. Ralchenko, J. Reader, and NIST ASD Team, NIST Atomic Spectra Database (version 5.12) (National Institute of Standards and Technology, Gaithersburg, USA), <https://dx.doi.org/10.18434/T4W30F>.
- [62] A. S. Kheifets, D. V. Fursa, and I. Bray, Two-electron photoionization of ground-state lithium, *Phys. Rev. A* **80**, 063413 (2009).
- [63] A. S. Kheifets, D. V. Fursa, C. W. Hines, I. Bray, J. Colgan, and M. S. Pindzola, Spin effects in double photoionization of lithium, *Phys. Rev. A* **81**, 023418 (2010).
- [64] A. S. Kheifets, D. V. Fursa, I. Bray, J. Colgan, and M. S. Pindzola, Differential cross sections of double photoionization of lithium, *Phys. Rev. A* **82**, 023403 (2010).
- [65] D. V. Fursa and I. Bray, Calculation of electron-helium scattering, *Phys. Rev. A* **52**, 1279 (1995).
- [66] D. V. Fursa and I. Bray, Convergent close-coupling calculations of electron scattering on helium-like atoms and ions: electron-beryllium scattering, *J. Phys. B: At. Mol. Opt. Phys.* **30**, 5895 (1997).
- [67] A. Müller, A. L. D. Kilcoyne, R. A. Phaneuf, K. Holste, S. Schippers, and A. S. Kheifets, Direct double ionization of the $\text{Ar}^+ M$ shell by a single photon, *Phys. Rev. A* **103**, L031101 (2021).
- [68] U. Fano, Effects of configuration interaction on intensities and phase shifts, *Phys. Rev.* **124**, 1866 (1961).
- [69] S. Schippers, Analytical expression for the convolution of a Fano line profile with a Gaussian, *J. Quant. Spectrosc. Radiat. Transfer* **219**, 33 (2018).
- [70] M. Togawa, S. Kühn, C. Shah, V. A. Zaytsev, N. S. Oreshkina, J. Buck, S. Bernitt, R. Steinbrügge, J. Seltmann, M. Hoesch, C. H. Keitel, T. Pfeifer, M. A. Leutenegger, and J. R. Crespo López-Urrutia, High-accuracy measurements of core-excited transitions in light Li-like ions, *Phys. Rev. A* **110**, L030802 (2024).
- [71] U. I. Safronova and V. S. Senashenko, The radiative decay of excited states of atomic systems with two K-shell vacancies, *J. Phys. B: At. Mol. Phys.* **10**, L271 (1977).
- [72] V. A. Zaytsev, I. A. Maltsev, I. I. Tupitsyn, and V. M. Shabaev, Complex-scaled relativistic configuration-interaction study of the LL resonances in heliumlike ions: From boron to argon, *Phys. Rev. A* **100**, 052504 (2019).
- [73] T. Pattard, A shape function for single-photon multiple ionization cross sections, *J. Phys. B: At. Mol. Opt. Phys.* **35**, L207 (2002).
- [74] M. F. Gu, The flexible atomic code, *Can. J. Phys.* **86**, 675 (2008).